V European Conference on Computational Fluid Dynamics
ECCOMAS CFD 2010
J. C. F. Pereira and A. Sequeira (Eds)
Lisbon, Portugal, 14–17 June 2010

SIMULATION OF BLOOD FLOW IN HUMAN AORTA INCLUDING THIRTEEN MAIN ARTERIES (ECCOMAS CFD 2010)

Erke Aribas[*†], Senol Piskin[†], and M.Serdar Celebi[†]

[†]Istanbul Tehcnical University
e-mail: erke.aribas, senol.piskin@be.itu.edu.tr, mscelebi@itu.edu.tr

Key words: Fluid Dynamics, hemodynamics, arterial tree, CFD

Abstract. *This paper investigates the mechanical properties of blood flow in main arterial system of human. The system includes aorta, subclavian, mesosentric, iliac artery, renal artery, celiac artery. The geometric domain of artery network is obtained using a real patient data. As an input, Womersley velocity profile [2] is used. Combination of thirteen arteries with aorta gives better understanding of the interactions of blood flow among the arteries. For example, the effect of a narrowing region at the iliac artery to the flow at aorta or renal artery can be studied with the help of the model presented. Results of the study include velocity, pressure and WSS (Wall Shear Stress) distributions at the arteries and the bifurcation regions of the arterial tree [1, 3]. Later, regional domains are inter-examined and dynamics of the system is compared within the thirteen branched model results.*

1 INTRODUCTION

Today, medical imaging methods such as CT and MRI are common, reliable and unavoidably useful in medical related fields. Although the technological growth is advancing in a rapid fashion, these methods are rarely used in obtaining data for further imaging and modeling analysis. To achieve this task, software based 3D modeling in which arterial bifurcations are restructured, is required.

The main purpose of this work is to simulate the blood flow using 13 branches of the most crucial and largest arteries in the chest and abdominal region of a human. It's thought as arteries and veins as simple tubes, so the artery is susceptible to biomechanical factors. Although the link between these factors and cardiovascular health are known for centuries through the cause of arterial diseases (e.g., see Young [1], who considered the hemodynamic properties, or Roy[2], who considered wall mechanics), it is understood barely today (Davies [3]). Our focus here is arterial trees and their relation between the circulation systems which are constantly being researched in order to find substitutes clinically [4].The branching systems start with a large diameter and continue with many smaller branches in the arterial system [6]. Further analysis on arterial physiology and hemodynamics can be found in Nichols and O'Rourke [7]. Recent advances in modeling of complex geometries of the arterial system introduces new understanding of artery wall mechanics which is crucial in advancing of the circulation of blood in arteries(e.g. [8,9]). Therefore, simulation in disease progression and clinical intervention are associated within artery wall mechanics. The approach taken in order to simulate diameter-defined artery trees started with one-element based modeling [4].

Atherosclerosis results from the chronic buildup of fatty material within the intimae layer. Highly risked factors can affect all arteries of the body, yet atherosclerosis tends to localize at branches and bends within the arterial tree. This usually leads to the formation of atherogenesis in local arteries [10–12].

To obtain actual patient arterial geometry, Mimics [13] software where all sliced images from a patient is used as an input. These images are gathered on top of each other to form the 3D design. Filtering of the arterial tree sections from this group of images leads to structuring a geometric model, which is created as a surface, using triangle cells. However, in order to simulate a flow model, geometry has to be filled with volumetric cells. This step is achieved by using volumetric mesh generation technique. Refinements and smoothing methods are inserted in and several modifications are added as the next step. Expanding the mesh into several numbered volumes is also analyzed since it may lead to a better understanding of the geometry. The artery tree is structured on an open artery model. Arterial system includes aorta, iliac artery, renal artery, subclavian, mesosentric, celiac artery etc. Preprocessing methods are then followed by applying CFD solver to the grid.

2 MODELING GEOMETRY

The paper must be written in English within a printing box of 16 cm x 24 cm, centered in the page. The paper including figures, tables and references must have a minimum length of 4 pages and must not exceed 20 pages. Maximum file size is 6 MB.

Patient is a 56 year old female and her data was obtained during a periodical check-up routine. Data is 512 by 512 CT (Computed Tomography) and the slices are 0.82

millimeter apart from each other. Certain protocols are applied such as preparation of the subject and scanning of the data. Preparation requires for the subject to remove all the metal related materials such as proteases. The most crucial section is making the subject move as little as possible. Scanning of data is achieved best when gantry tilt angle is absolute zero. Quality of the images varies according to gantry tilt angle and images with higher angle produce less quality images.

Linear transformation of these image based pixels is represented in Hounsfield [13] unit scale in which radio-density of distilled water at standard pressure and temperature is defined as zero Hounsfield units. The scaling is used to separate arteries from bone and other soft tissues and application of this method can be seen in Figure 1a and 1b. After connecting sliced images as voxels, morphology and region growing techniques are employed using graphics software. Depending on the quality of the data, these methods take a serious time. When arteries and soft tissues are inseparable by the software at first, additional technical operations are needed such as the operations in Figure 1c.

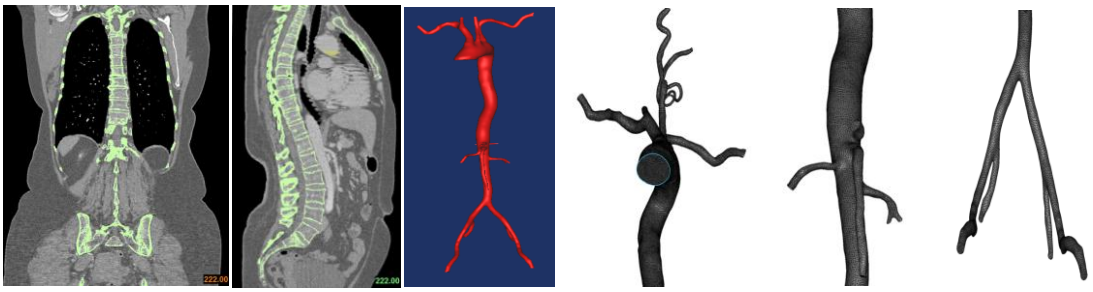

a b c d e f

Figure 1: Reconstructed images of STL (stereo-lithography) converted meshes. a) creating inlet and outlet sections with dense meshes b) interior volume creation. c) marking of troubled cells. Obtaining of 13 branch artery bifurcations with the help of Hounsfield measures. d) coronal e) sagittal f) 3D reproduction. The steps are already achieved with results in previous studies. [23]

Remeshing techniques are applied in order to construct 13 branch geometry. Since 3D object is quite coarse, quality check of the mesh is needed. In order to achieve continuity of mass, dense meshes in the inlet and the outlet sections are implemented.

The geometry involves multiple enclosures connected via smaller-diameter pipes of arteries, leading pressure levels in all. This may result one of the zones becoming quite large compared to other sections. Double precision calculations may, therefore, be necessary not only to resolve the pressure differences that drive the flow, but also the velocity flow at the inlet, since these will typically be much smaller than the pressure and velocity levels. As it can be seen from figure 1d through 1e, due to the inefficient transfer of boundary information, convergence and/or accuracy may be critical in solving the flow simulations.

3 HEMODYNAMICS.

Since the pioneering work of Perktold et al. [14], much of the research in modeling blood flow in human arteries has focused on the solution of the three-dimensional

equations using numerical methods, particularly finite elements. Such methods are well suited to the investigation of phenomena difficult to describe using in vitro techniques, including wall compliance [15,16], mass transport [17], and realistic anatomic models [18]. An overview of contemporary experimental and computational methods for quantifying hemodynamics can be found in Taylor and Draney [19].

Navier-Stokes Equations is stated as,

$$\rho\frac{Du}{Dt} = -\frac{\partial p}{\partial x} + \frac{\partial p}{\partial x}\left[2\mu\left(\frac{\partial y}{\partial x} + \lambda divu\right)\right] + \frac{\partial}{\partial y}\left[\mu\left(\frac{\partial u}{\partial y} + \frac{v}{x}\right)\right] + \frac{\partial}{\partial z}\left[\mu\left(\frac{\partial u}{\partial z} + \frac{\partial w}{\partial x}\right)\right] + S_{M_x}$$

$$\rho\frac{Dv}{Dt} = -\frac{\partial p}{\partial y} + \frac{\partial}{\partial x}\left[\mu\left(\frac{\partial u}{\partial y} + \frac{\partial v}{\partial x}\right)\right] + \frac{\partial}{\partial y}\left[2\mu\left(\frac{\partial v}{\partial y} + \lambda divu\right)\right] + \frac{\partial}{\partial z}\left[\mu\left(\frac{\partial v}{\partial z} + \frac{\partial w}{\partial y}\right)\right] + S_{M_y}$$

$$\rho\frac{Dw}{Dt} = -\frac{\partial p}{\partial z} + \frac{\partial}{\partial x}\left[\mu\left(\frac{\partial u}{\partial z} + \frac{\partial w}{\partial x}\right)\right] + \frac{\partial}{\partial y}\left[\mu\left(\frac{\partial v}{\partial z} + \frac{\partial w}{\partial y}\right)\right] + \frac{\partial}{\partial z}\left[2\mu\left(\frac{\partial w}{\partial z} + \lambda divu\right)\right] + S_{M_z}$$

The following boundary conditions were applied: It is assumed there is no slip on the wall, it is applied zero pressure gradient on the wall, Womersley velocity profile is given at velocity inlet, in this case transient velocity profile is used.

An unsteady simulation is performed on the 13 branch geometry. The system includes aorta, iliac artery, renal artery, and celiac artery etc. There are one inlet and 13 outlets in the model and the laminar flow is induced at the inlet. Flow patterns are taken from celiac artery (middle torso) where geometry differences highly change the outlet velocity values. The velocity profiles can be seen vividly in figure 6 below in scaling colors.

The simulations show velocity profiles starting from the aorta ranging around 1 m/s and going up 2-2.5 m/s in the carotid artery section can be seen from figure 3 b. Also what can be seen from iliac and renal sections of the arteries which are in figure 3 a and 3 c is the increase of velocity profiles in the narrow arteries. This is continuing to increase when the blood particle travels further and up to 4 times magnitude of the inlet velocity is detected.

A Womersley number is a dimensionless number in biofluid mechanics and a dimensionless expression of the of pulsatile flow frequency in relation to viscous effects.

$$w(r,t) = \frac{2B_0}{\pi R^2}\left[1 - \left(\frac{r}{R}\right)^2\right] + \sum_{n=1}^{N}\left[\frac{B_n}{\pi R^2}\left[\frac{1 - \frac{J_{0\left(a_n \frac{x}{R} j^{3/2}\right)}}{J_0\left(a_n j^{3/2}\right)}}{1 - \frac{2J_1\left(a_n x^{3/2}\right)}{a_n j^{3/2} J_0\left(a_n j^{3/2}\right)}}\right]\right]$$

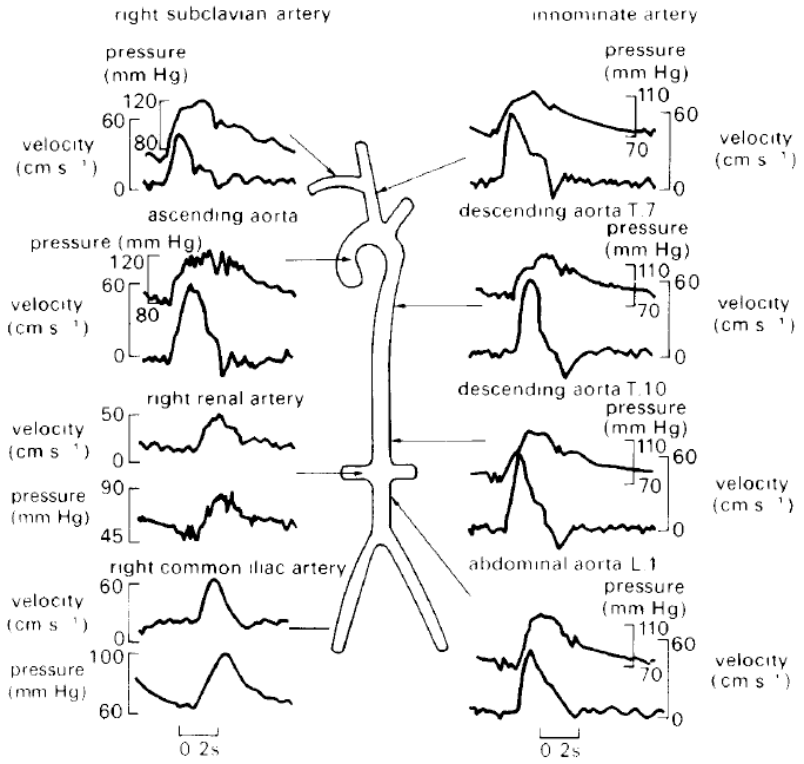

Figure 2: Pressure and velocity pulse waveforms in the aorta and arterial branches of a dog. Note that the pressure maximum becomes amplified while the velocity maximum decreases as the blood moves downstream. (From Caro et al 1978, The Mechanics of the Circulation; reprinted by permission of Oxford University Press.)

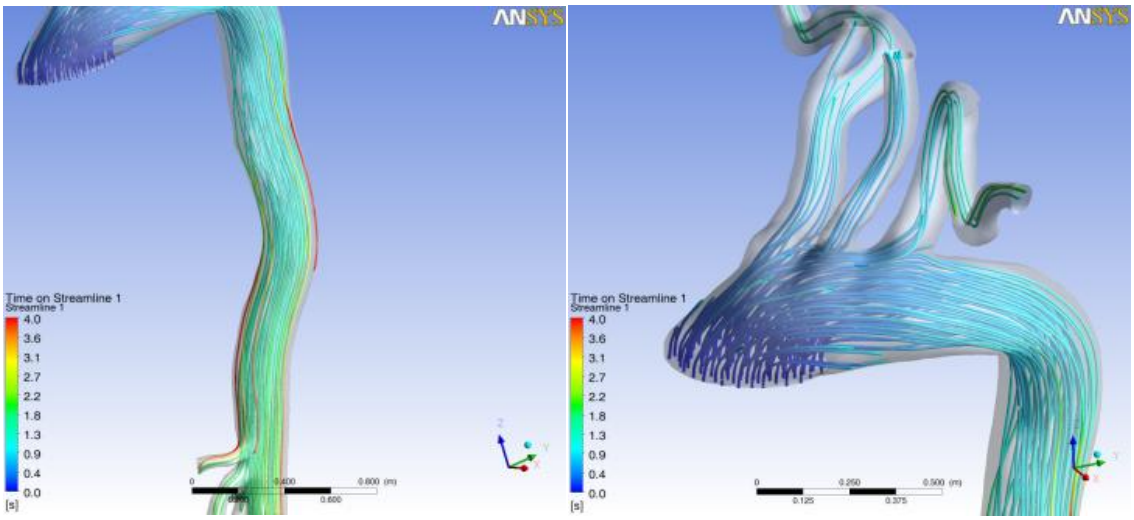

a b

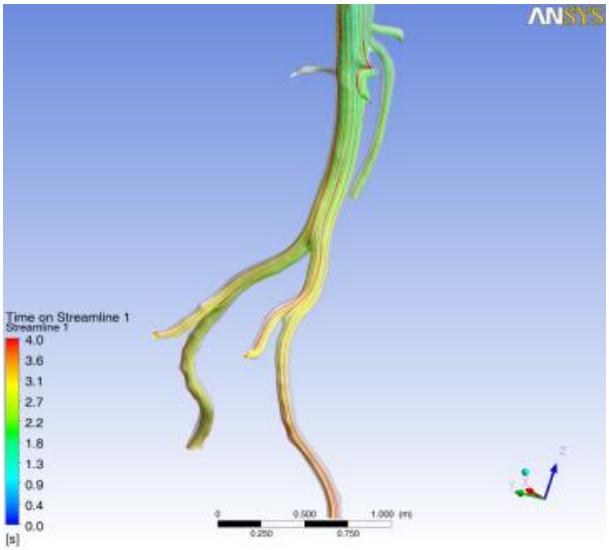

c

Figure 3: a) Velocity lines of abdominal artery b) Velocity lines of the outlet. c) Velocity lines in the iliac arteries. Greener lines show faster flow velocity where red lines show the greatest velocities

The Womersley number arises in the solution of the linearized Navier Stokes equations for oscillatory flow (presumed to be laminar and incompressible) in a tube [20]. Our previous work included three dimensional transient simulations of the carotid artery with a fixed diameter tube [21]. In this study, the entire blood network model is partitioned into three main sections which are renal, aortic and iliac regions and show geometrical models in details below in figure 4 a,b and c.

Simulation results are taken in three and one dimensional data in order to achieve clarity. One dimensional graphs are velocity versus distance graphs that are taken from aorta inlet and outlet from renal and iliac arteries. This constitutes better comparison between one dimensional and three dimensional results.

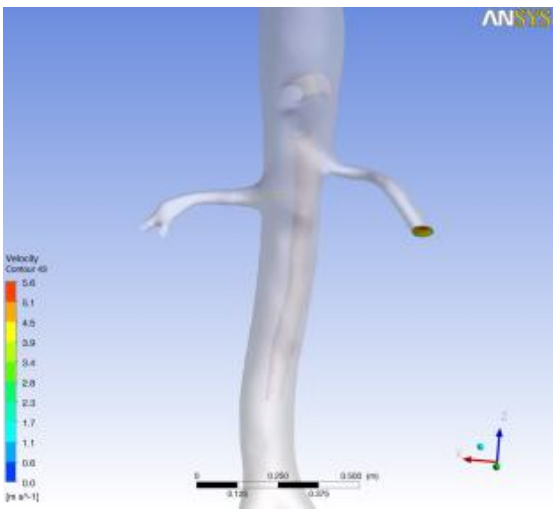

a

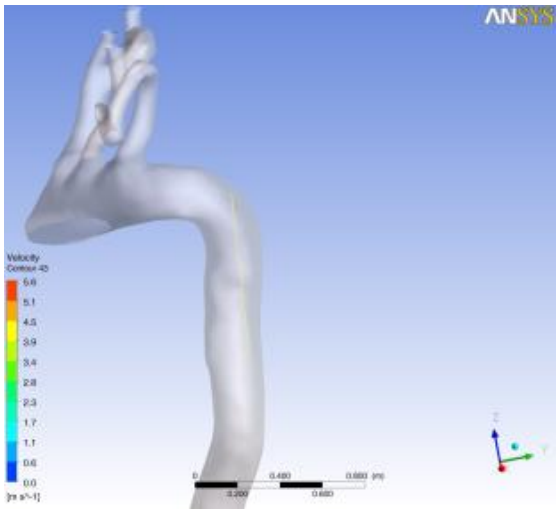

b

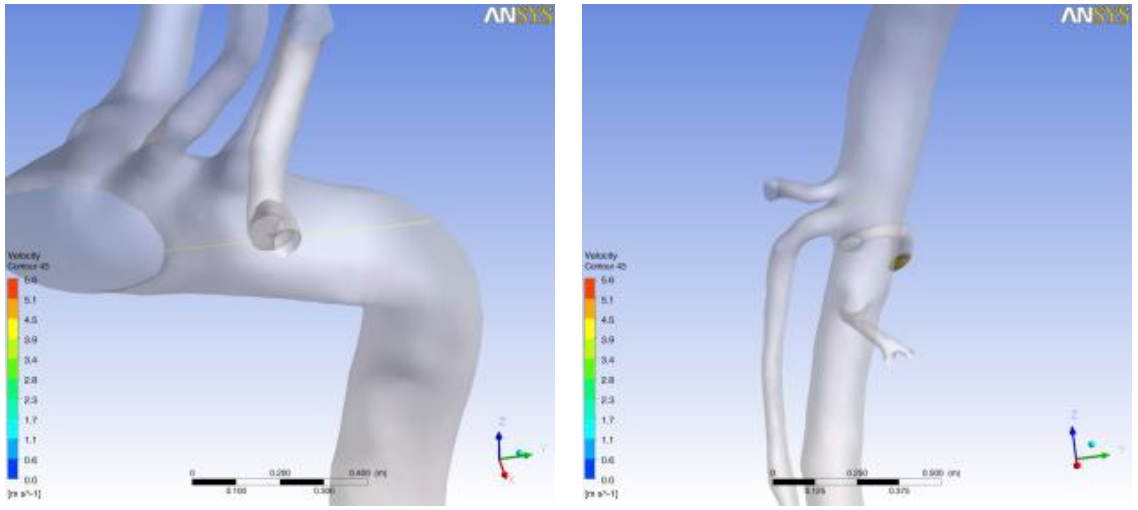

c d

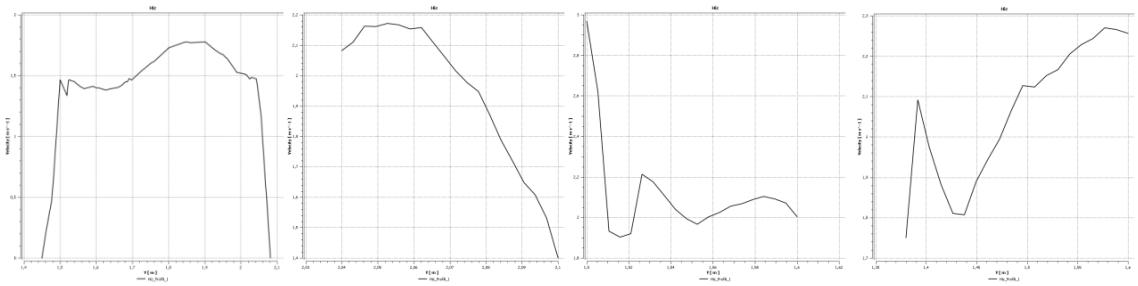

e f g h

Figure 4: a) Velocity lines of abdominal renal artery b) Velocity lines in the aortic region. c) Velocity lines in the aortic region. d) Velocity lines in the iliac arteries. e-f) Velocity-distance data where vertical axis is velocity and horizontal axis is the diameter of corresponding inlet or the outlets from sections a to d in one-dimensional representation.

One dimensional graphics is a good way to validate the results although the simulations are handled in three dimensional. Our inlet velocity is in the form of Womersley profile and one dimensional graphic (figure 4g) fairly represents a similarity of this behavior.

3.1 Pressure Distribution

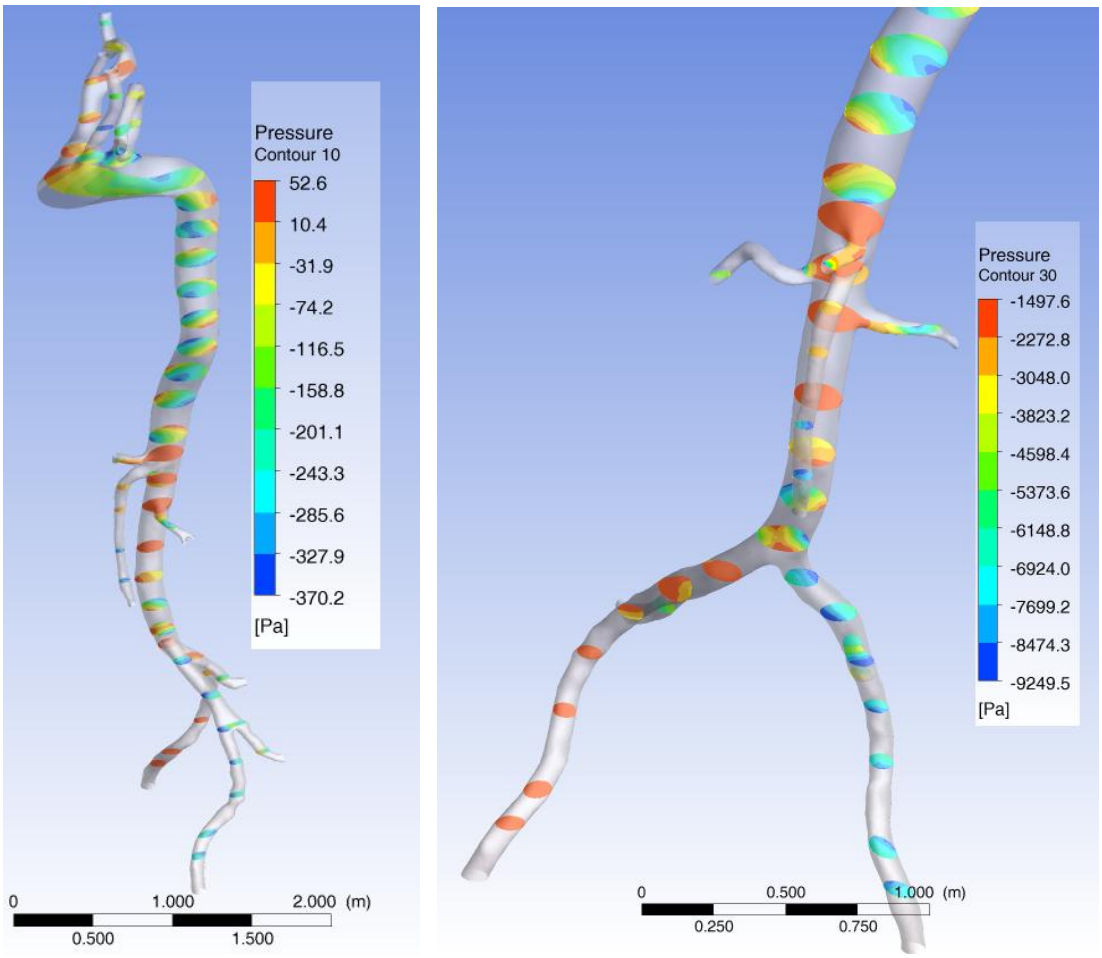

a b

Fig.8. a) Total pressure values for the patient - specific in the entire model b) total pressure values in the abdominal aorta, renal and the iliac region (Fig. 3 a, b and c).

4 CONCLUSION

The main headings should be written left aligned, in 12pt, boldface and all capital Roman letters. There should be a 12pt space before and 6pt after the main headings.

Results show that better representation of complex 13 artery bifurcation geometry gives more detail on the flow characteristic hinting us the flow projections of a nozzle effect(see figure 8) and high pressure increment at the level 2 bifurcation in the iliac. These effects of results were also noticed in previous studies [22].

The narrowing of the arteries in the celiac region happens to show high speed and pressure values in the results. This is referred to as stenosis. The velocity vectors indicate that multiple layers of the wall Conversion of scanning to a geometrical model needs to be generated with as much as data (nodes or volumes) possible but there are many parameters that may be effective before construction of the geometry such as procurement of data and patient status.

The velocity differences seen in periods of 0.2 second intervals show that Womersley wave profile changes rapidly when blood streams from aorta through the thinner arteries such as iliac and renal.

In this study, our model is based on an open loop circulation where blood is applied into the aorta inlet and the outlet sections do not send any information nor update of such property like velocity or pressure. Further studies are likely to be focused on closed loop modeling in which blood flow circulation is simulated with passing of mechanical properties between inlet and the other 13 outlets. Further research may also include investigating medical anomalies like abdominal aortic aneurysms (AAA) especially in the meso-centric aorta region.

5 ACKNOWLEDGEMENTS

Authors thank to UYBHM (National High Performance Computing Center) at Istanbul, Turkey for computing resources.

REFERENCES

[1] T. Young, Hydraulic investigations, subservient to an intended cronian lecture on the motion of the blood, Philos. Trans. Roy. Soc. (London) 98 (1808) 164–186.
[2] C.S. Roy, The elastic properties of the arterial wall, J. Physiol. 3 (1881) 125–159.
[3] P.F.Davies, "Spatial Hemodynamics, the Endothelium, and FocalAtherogenesis: A cell Cycle Link?" Circ. Res, vol 86, no.2, 2000, pp. 114-116.
[4] A.R. Pries, T.W. Secomb, P. Gaehtgens, Design principles of vascular beds, Circ. Res. 77 (5) (1995) 1017–1023.
[5] M.S. Olufsen, Structured tree outflow condition for blood flow in larger systemic arteries, Am. J. Physiol. 276 (1 Pt 2) (1999) H257–H268.
[6] G.S. Kassab, C.A. Rider, N.J. Tang, Y.C. Fung, Morphometry of pig coronary arterial trees, Am. J. Physiol. 265 (1 Pt 2) (1993) H350–H365.
[7] W.W. Nichols, M.F. O'Rourke, Mcdonald's Blood Flow in Arteries: Theoretical, Experimental and Clinical Principles, fifth ed., Oxford University Press, 2005.
[8] K.S. Burrowes, P.J. Hunter, M.H. Tawhai, Anatomically based finite element models of the human pulmonary arterial and venous trees including supernumerary vessels, J. Appl. Physiol. 99 (2) (2005) 731–738.
[9] R.L. Spilker, J.A. Feinstein, D.W. Parker, V.M. Reddy, C.A. Taylor, Morphometry based impedance boundary conditions for patient-specific modeling of blood flow in pulmonary arteries, Ann. Biomed. Engrg. 35 (4) (2007) 546–559.
[10] C.G. Caro, J.M. Fitz-Gerald, R.C. Schroter, Atheroma arterial wall shear.
Observation, correlation and proposal of a shear dependent mass transfer mechanism for atherogenesis, Proc. Roy. Soc. London B: Biol. Sci. 177 (46) (1971) 109–159.
[11] M.H. Friedman, G.M. Hutchins, C.B. Bargeron, O.J. Deters, F.F. Mark, Correlation between intimal thickness and fluid shear in human arteries, Atherosclerosis 39 (3) (1981) 425–436.
[12] C.K. Zarins, D.P. Giddens, B.K. Bharadvaj, V.S. Sottiurai, R.F. Mabon, S. Glagov, Carotid bifurcation atherosclerosis. Quantitative correlation of plaque localization with flow velocity profiles and wall shear stress, Circ. Res. 53 (4) (1983) 502–514.
[13] Hounsfield, G N, Computed Medical Imaging, Science/AAAS 3 science.6997993 October 1980: 22-28: 10.1126/

[14] K. Perktold, M. Resch, R.O. Peter, Three-dimensional numerical analysis of pulsatile flow and wall shear stress in the carotid artery bifurcation, J. Biomech. 24 (6) (1991) 409–420.
[15] C.A. Figueroa, I.E. Vignon-Clementel, K.C. Jansen, T.J.R. Hughes, C.A. Taylor, A coupled momentum method for modeling blood flow in three-dimensional deformable arteries, Comput. Methods Appl. Mech. Engrg. 195 (41–43) (2006) 5685–5706.
[16] K. Perktold, G. Rappitsch, Computer simulation of local blood flow and vessel mechanics in a compliant carotid artery bifurcation model, J. Biomech. 28 (7) (1995) 845–856.
[17] C.R. Ethier, Computational modeling of mass transfer and links to atherosclerosis, Ann. Biomed. Engrg. 30 (4) (2002) 461–471.
[18] C.A. Taylor, T.J.R. Hughes, C.K. Zarins, Finite element modeling of blood flow in arteries, Comput. Methods Appl. Mech. Engrg. 158 (1998) 155–196.
[19] C.A. Taylor, M.T. Draney, Experimental and computational methods in cardiovascular fluid mechanics, Annu. Rev. Fluid Mech. 36 (2004) 197–231.
[20] Womersley JR (March 1955). "Method for the calculation of velocity, rate flow, and viscous drag in arteries when the pressure gradient is known". J Physiol. 127 (3): 553–563. PMID 14368548. PMC 1365740.
[21] Piskin, S, Celebi, MS, A Carotid Artery Bifurcation Modelling for Blood Flow, Seventh Triennial International Symposium on Fluid Control, Measurement and Visualization (FLUCOME'03), Sorrento, Italy, 2003.
[22] Aribas. E, Veeckmans. B, Celebi. MS,A Study on 3D Blood Flow Simulation in Human Carotid Artery Bifurcations Innovations in Computer Aided Engineering Mimics Mimics Innovation Awards 2008.
[23] Aribas, E. S.Piskin M.S. Celebi 3D Blood Flow Simulations in Human Arterial Tree Bifurcations BIYOMUT 2009. 14th National. 2009 İzmir, Turkey